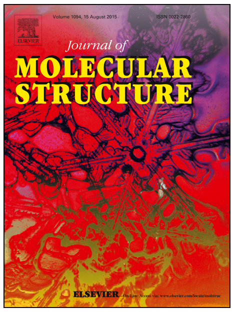

Synthesis and spectroscopic characterization of Ni(II) complexes involving functionalised dithiocarbamates and triphenylphosphine: anagostic interaction in (N-cyclopropyl-N-(4-fluorobenzyl)dithiocarbamato-S,S')- (thiocyanato-N)(triphenylphosphine)nickel(II)

E. Sathiyaraj, T. Srinivasan, Dr. S. Thirumaran, D. Velmurugan

PII: S0022-2860(15)30241-6
DOI: 10.1016/j.molstruc.2015.08.053
Reference: MOLSTR 21785

To appear in: *Journal of Molecular Structure*

Received Date: 3 April 2015
Revised Date: 19 August 2015
Accepted Date: 25 August 2015

Please cite this article as: E. Sathiyaraj, T. Srinivasan, S. Thirumaran, D. Velmurugan, Synthesis and spectroscopic characterization of Ni(II) complexes involving functionalised dithiocarbamates and triphenylphosphine: anagostic interaction in (N-cyclopropyl-N-(4-fluorobenzyl)dithiocarbamato-S,S')-(thiocyanato-N)(triphenylphosphine)nickel(II), Journal of Molecular Structure (2015), doi: 10.1016/j.molstruc.2015.08.053.

GRAPHICAL ABSTRACT

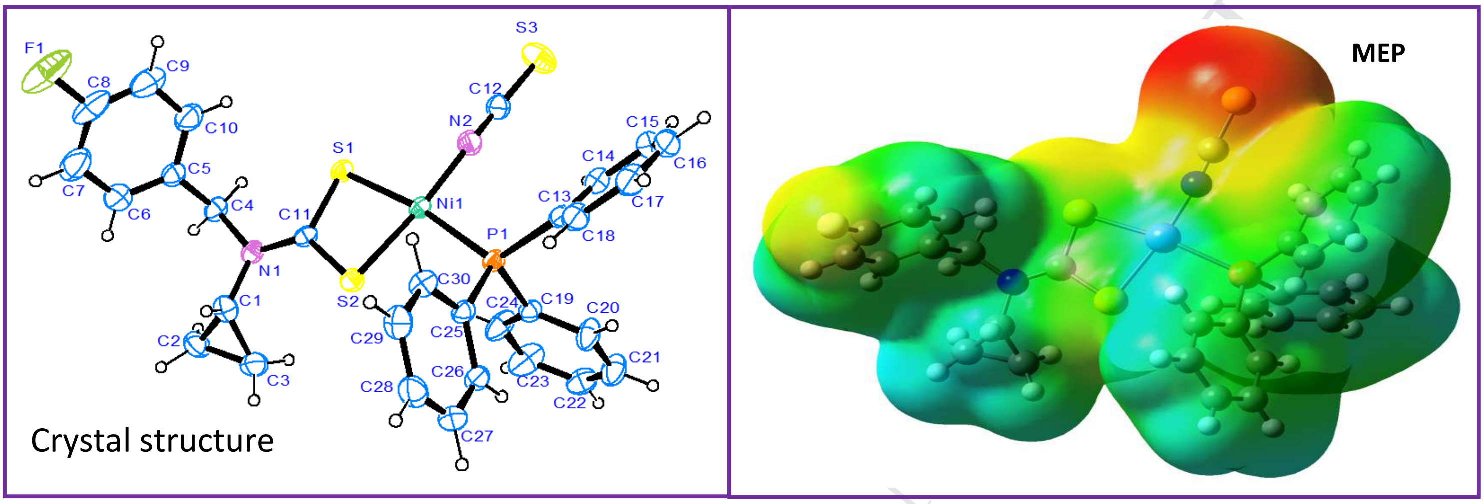

Synthesis and spectroscopic characterization of Ni(II) complexes involving functionalised dithiocarbamates and triphenylphosphine: anagostic interaction in (N-cyclopropyl-N-(4-fluorobenzyl)dithiocarbamato-S,S′)-(thiocyanato-N)(triphenylphosphine)nickel(II)

E. Sathiyaraj[a], T. Srinivasan[b], S. Thirumaran[a]* and D. Velmurugan[b]

[a]*Department of Chemistry, Annamalai University, Annamalinagar 608 002, Tamilnadu, India.*

[b]*Centre of Advanced Study in Crystallography and Biophysics, University of Madras, Maraimalai Campus (Guindy Campus), Chennai 600 025, India*

*Address for correspondence

Dr. S. Thirumaran
Department of Chemistry
Annamalai University
Annamalainagar 608 002
Tamilnadu, INDIA
Tel: +91 9842897597
E-mail: sthirumaran@yahoo.com

Synthesis and spectroscopic characterization of Ni(II) complexes involving functionalised dithiocarbamates and triphenylphosphine: anagostic interaction in (N-cyclopropyl-N-(4-fluorobenzyl)dithiocarbamato-S,S′)-(thiocyanato-N)(triphenylphosphine)nickel(II)

E. Sathiyaraj[a], T. Srinivasan[b], S. Thirumaran[a]* and D. Velmurugan[b]

ABSTRACT

Twelve new nickel(II) complexes namely $[Ni(S_2CNRR')_2]$**(1-6)** and $[Ni(S_2CNRR')(NCS)(PPh_3)]$**(7-12)** [where R=cyclopropyl (^{c}Pr); R'=2**H**O–C_6H_4–CH_2– **(1,7)**, 3**H**O–C_6H_4–CH_2– **(2,8)**, 4**H**O–C_6H_4–CH_2– **(3,9)**, 4C**H₃**O–C_6H_4–CH_2– **(4,10)**, 4F–C_6H_4–CH_2– **(5,11)**, 4Cl–C_6H_4–CH_2– **(6,12)**] have been prepared and characterized by elemental analysis, IR, UV-Vis and NMR (^{1}H and ^{13}C) spectroscopy. A single crystal X-ray structural analysis was carried out for (N-cyclopropyl-N-(4-fluorobenzyl)dithiocarbamato-S,S′)(thiocyanato-N)-(triphenylphosphine)nickel(II). The increase in wavenumber of $\nu_{C\text{-}N}$ thioureide and decrease in chemical shift values of heteroleptic complexes **7-12** compared to that of homoleptic complexes **1-6** are due to the mesomeric drift of electron density from the dithiocarbamate moiety towards the metal centre, increasing the carbon-nitrogen double bond character. The increased strength of C−N bond is due to the presence of the π-accepting triphenylphosphine. Electronic spectral studies indicated square planar geometry around the nickel(II) central atom for all the complexes. Single crystal X-ray structural analysis of **11** confirms that the coordination geometry about the Ni is distorted square planar. The C−H···F interactions lead to a polymeric structure and a rare intramolecular anagostic interaction [M···H= 2.929 Å] is observed. The molecular geometry, HOMO-LUMO in the ground state and MEP have been calculated for **11** using the Hartree-Fock (HF) method with the LANL2DZ basic set. The optimized bond lengths and bond angles agree well with the experimental results. The asymmetry in the Ni−S bonds reveal the greater trans influence of triphenylphosphine compared to that of the isothiocyanate ion.

Keywords: Nickel(II) dithiocarbamate; FT-IR; UV-Vis; NMR; Anagostic interaction

INDRODUCTION

The current interest in the study of the chemistry of transition metal dithiocarbamate complexes is motivated by their utility in a diverse applications, such as in medicine [1-4], agriculture [5-7], organic synthesis [8] and even as synthetic precursor for metal sulfide nanoparticles [9-15]. In addition to this, considerable interest was also for the X-ray crystallographic studies of transition metal complexes, and there is a wealth of structural data available for these complexes, with some notable studies motivated by crystal engineering [16-18]. Many metal dithiocarbamate complexes are stabilized by C−H···S, C−H···O, C−H···N, C−H···π and π−π interactions providing 3D, 2D and 1D supramolecular structures [19, 20]. The functionalizaton of N-bound organic moiety in the dithiocarbamate ligand may generate a variety of molecular architectures and potentially gives rise to tunable physical properties [21]. One commonly known functionalized dithiocarbamate ligand is N,N-di(2-hydroxyethyl)dithiocarbamate which exhibits different supramolecular aggregation in its complexes [22, 23].

In addition to these interactions, some homoleptic and heteroleptic dithiocarbamate complexes of group 10 metal ions exhibited the rare C−H···M intramolecular anagostic interactions [24-29]. Recently, C−H···Ni intermolecular anagostic interactions in some nickel-bis dithiocarbamate complexes have been reported [30, 31]. This anagostic interactions (H···Ni distance between ≈2.3-2.9 Å) are believed to be important for catalytic applications [32]. In recent years, scientists used computational methods to characterize the complexes because of their good efficiency and great precision in the prediction of a number of molecular properties [33]. Computational studies also help to evaluate compound properties economically and to clarify some experimental phenomena insightfully [34, 35]. Due to the applications of metal dithiocarbamate complexes and their diverse supramolecular aggregation patterns, we thought it is worth to study the synthesis and characterization of some new homoleptic and heteroleptic Ni(II) complexes involving functionalized dithiocarbamate ligands.

Experimental

All materials and solvents were obtained from commercial suppliers and used without further purification. Melting points were determined on an electro thermal melting point apparatus and were reported uncorrected. Elemental analysis was performed in a varioMICRO V2.2.0 apparatus. Infrared spectra were recorded on a SHIMADZU FT-IR spectrophotometer in the frequency range 4000–400 cm^{-1}. ^{1}H NMR spectra were recorded on Bruker 400 MHz and the ^{13}C NMR spectra on a Bruker 100 MHz spectrometer using $CDCl_3$ and DMSO-d_6 as solvents and tetramethylsilane (TMS) as internal standard. Single-crystal X-ray structural studies were performed on a bruker SMART APEXII Diffractometer. The intensity data were collected at 293(2) K using graphite monochromated Mo Kα radiation (λ = 0.71073 Å). The structure was solved by the direct method and refined using the SHELX-97 [36, 37] suite of programs. Figures were drawn using ORTEP-3.2 and MERCURY-2.3. The hydrogen atoms were included at geometrically calculated positions in the final stages of the refinement and were refined according to the ‘‘riding model”. All non-hydrogen atoms were refined anisotropically. All calculations were performed with GAUSSIAN09 program package [38] with the aid of the GaussView visualization program. All the characterization data are given in supplementary material.

EXPERIMENTAL

Preparation of amines

4.6 mmol of cyclopropylamine and 5.1 mmol of substituted benzaldehydes (2-OH, 3-OH, 4-OH, 4-OCH_3, 4-F and 4-Cl) were dissolved in methanol (30 mL) and the solution was stirred for 2 h at room temperature. The solvent was removed by evaporation. The resulting colourless oil was dissolved in methanol-dichloromethane solvent mixture (1:1, 20 mL) and sodium borohydride (13.8 mmol) was added slowly at 5°C and stirred for 2 h before removal of ice bath. The reaction mixture was stirred at room temperature for 20 h. After evaporation of the solvent, the resulting viscous liquid was washed with water, and dichloromethane was added in order to extract the product. Evaporation of the organic layer gave N-cyclopropyl-N-substituted benzylamine as a pale yellow oil

Preparation of complexes (1-6)

N-cyclopropyl-N-substituted benzylamine (4.0 mmol) in ethanol was mixed with carbon disulfide (4.0 mmol) under ice cold condition. To the resultant yellow dithiocarbamic acid solution, aqueous solution of $NiCl_2 \cdot 6H_2O$ (2.0 mmol) was added with constant stirring. The solid which precipitated was washed several times with cold water and then dried. (**Fig. 1**)

Preparation of complexes (7-12)

A mixture of complex (**1-6)** (1.0 mmol, 0.624 g), PPh_3 (2.0 mmol, 0.524 g), $NiCl_2 \cdot 6H_2O$ (1.0 mmol, 0.237 g) and NH_4SCN (2.0 mmol, 0.152 g) was refluxed for 3 h in acetonitrile-methanol solvent mixture (1:1, 50 mL). The purple-red solution obtained was filtered and left for evaporation. After 2 days, a purple-red solid separated out which was recrystallized from dichloromethane. (**Fig. 1**)

Results and discussion

IR spectral studies

Important absorptions in the dithiocarbamate complexes are due to $\nu_{C–N}$ and $\nu_{C–S}$ stretching modes [39-42]. For the homoleptic complexes (**1–6)**, strong bands appeared in the 1470-1474 cm^{-1} region that are due to $\nu_{C–N}$ (thioureide). For the heteroleptic complexes (**7-12**), ν_{C-N} (thioureide) bands were observed in the 1474-1491 cm^{-1} region. The increase in wavenumber for complexes (**7-12**), compared to that of the parent complexes (**1-6**), is attributed to the mesomeric drift of electron density from dithiocarbamate ligand to nickel through the thioureide C-N bond [43]. The $\nu_{C–S}$ stretching vibrations are observed around 1000 cm^{-1}, without any splitting, supporting the bidentate coordination of the dithiocarbamate ligand [44]. The observed stretching frequencies around 2088 cm^{-1} are due to the 'N'-coordinated isothiocyanate anion.

Electronic spectral studies

Electronic spectra of the prepared complexes **1-12** support the assumption of the square planar coordination of nickel(II) central atom [45, 46]. In all the complexes, the bands observed below 350 nm are due to the intraligand π-π* transitions. In addition to the charge transfer bands, the bands observed in the range of 425-650 nm are due to the d-d transitions. In Complexes **1-6**, two bands are observed around 620 and 460 nm. These bands correspond to $d_{xy} \rightarrow dx^2–y^2$ and $dz^2 \rightarrow dx^2–y^2$ transitions, respectively. A band observed around 483 nm for the heteroleptic complexes (**7-12**) are due to d-d transitions. These bands are assigned to $dz^2/dxy \rightarrow dx^2–y^2$ transitions.

NMR spectral studies

^{1}H NMR spectral studies

In the complexes **1-6**, the methylene protons of benzyl and methyne protons of cyclopropyl group give signals around 4.66 and 2.60 ppm, respectively. The remaining signals in the aliphatic region are assigned to the methylene protons of cyclopropyl group. The methylene protons and methyne proton adjacent to nitrogen atom are greatly deshielded and are observed in the downfield region due to complexation. For all the complexes, the signals observed in the downfield region, 6.64-7.71 ppm, are due to the aromatic protons in the dithiocarbamate and triphenylphosphine ligands. Aliphatic proton signals in heteroleptic complexes **7-12** appeared as broad signals. The fast isothiocyanate ligand exchange process is responsible for the broadening of the aliphatic proton signals [47]. A singlet observed around 9.80 ppm in complexes **1-3** is assigned to OH protons. A signal is expected for OH proton in complexes **7-9**. But this signal is merged with aromatic proton signals of dithiocarbamate and triphenylphosphine ligands. Complexes **4** and **10** exhibit a singlet around 3.8 ppm due to methyl protons of the methoxy group.

^{13}C NMR spectral studies

All the complexes show a single downfield resonance characteristic of NCS_2 carbon of dithiocarbamate ligands in the range 206.1-213.1 ppm [48]. The upfield shift in the NCS_2 chemical shift values of heteroleptic complexes (**10-12**) compared to that of homoleptic complexes (**4-6**) is due to the mesomeric drift of electron density from the dithiocarbamate moiety towards the metal centre, increase the carbon nitrogen double bond character. This observation reveals that the increased strength of the thioureide bond is due to the presence of π-accepting phosphine. In all the complexes **1-12,** the signals for methylene carbon of benzyl group and methyne carbon of cyclopropyl group appear around 51.8 and 31.6 ppm, respectively. The remaining signals in the aliphatic region are assigned to the methylene carbon of cyclopropyl group. In all the cases, aromatic carbon signals appear in the region 113.8-163.9 ppm. A weak signal observed in the downfield region 154.8-159.6 ppm for complexes **1-4** and

7-10 is due to the *ipso* carbon of the dithiocarbamate ligand. In the case of complexes **9** and **10**, the thiocyanate (NCS) carbon resonates around 143 ppm. In the fluoro-substituted complexes **5** and **11**, two signals appeared around 161 and 164 ppm that are due to the *ipso* carbon [49].

Crystal structure

We prepared Ni(II) complexes containing functionalized dithiocarbamate ligands to study the intra-and intermolecular interactions due to the presence of a functional group on the phenyl ring. Most of the samples gave rise to the plates upon recrystalisation, and these crystals proved to be unsuitable for single crystal X-ray structural analysis. Crystals suitable for single crystal X-ray structure determination were obtained only for complex **11.**

The ORTEP diagram of complex **11** is given in **Fig. 2.** Details of the crystal data and structure refinement parameters are summarized in **Table 1**. Selected bond lengths and angles are given in **Table 2**. Single crystals of complex **11** suitable for X-ray crystallography were obtained from dichloromethane: acetonitrile (2:1) solution. In this complex, the nickel(II) ion is coordinated to three ligands, two sulfur atoms from dithiocarbamate, one nitrogen from thiocyanate and one phosphorus from triphenylphosphine in a distorted square planar. The bond angles P1-Ni-S2= 92.73(4)°, N2-Ni-S1=93.45(10)°, and N2-Ni-P1=93.45(3)° are less distorted from 90° than S2-Ni-S1 angle, which is 78.55(4)°**.** The large deviation of the S2-Ni-S1 bond angle from 90° is due to the chelation of dithiocarbamate ligand. The structure adopted by this complex is characterized using τ_4–descriptor for four coordinated ions [50]. The distortion index is defind as $\tau_4 = (360-(\alpha+\beta))/141$. The τ_4 values for perfect tetrahedral, trigonal pyramid, seesaw structure and perfect square planar are 1.00, 0.85, 0.64-0.07 and 0.00, respectively. The τ_4 value of this complex (0.1249) indicates that the coordination geometry around Ni(II) is best described as being 12% along the pathway of distortion from the square planar toward seesaw structure (τ_4=0.64-0.07) .

The average Ni-S bond lengths, 2.2026(12) Å, are similar to those observed in other nickel dithiocarbamate complexes [51]. The Ni-S distance *trans* to the phosphorus is longer 2.2234(12) Å than those found in case of the *trans* to the NCS$^{\square}$ [Ni-S=2.1819 (11) Å]. This reflects the greater *trans* influence of triphenylphosphine compared to that due to the thiocyanate group. The short Ni-N2 [1.859(3) Å] and Ni-P1 [2.1991(12) Å] distances confirm the effective bonding of nickel to the thiocyanate and triphenylphosphine moieties. The N-C-S angle (178.6°) indicates a slight deviation from linearity. This is due to the both steric effect of the bulky triphenylphosphine and weak S···H-C (S···H=2.619 Å) interaction. A significant delocalization of the π-electron density over the S_2CN moiety in complex **11** is typical for bidentate coordination of any dithiocarbamate anion to a transition metal and is evident from the C-N and C-S bond length values (**Table 2**).

For complex **11**, in addition to the van der Waals interactions, the molecular structure is influenced by the intramolecular C-H···S hydrogen bond involving S1 (**Fig**. **3.**). The complex molecules are bonded to an neighbouring molecule through C3-H3···F and C1-H1···F interactions, resulting in a polymeric structure (**Fig. 4.).** Three forms of C-H···M interactions, namely: (i) hydrogen bond (ii) agostic and (iii) anagostic were reported [52, 53]. Hydrogen bonds are 3-centre-4-electron interactions with an almost linear geometry. Agostic interactions are 3-centre-2-electron interactions and characterized by the short M···H distance (≈1.8-2.2 Å) and C-H···M bond angles (90-130°). Anagostic interactions are largely electrostatic in nature and characterized by long M···H distance (≈2.3–2.9 Å) and large M···H-C bond angles (≈110-170°). The anagostic interactions are typically formed with group 10 metal ions with d^8 configurations

[54]. The packing, steric and electronic effects of both bulky ligands and diamagnetic nickel(II) d^8, forces the *ortho* proton of one of the phenyl ring of PPh_3 ligand to be in close proximity to one of the axial positions around the nickel. This creates an unusual anagostic interaction (**Fig**. **5**) and is observed in **11** (M···H=2.929 Å and <M···H-C=117.13°). Anagostic and C-H···F (polymeric structure) interactions are absent in (N-cyclopropyl-N-benzyldithiocarbamato-S,S′)(thiocyanato-N)(triphenylphosphine)nickel(II)[55].

This results show that the interactions observed in the complex **11** are mainly due to the presence of fluorine on the *para* position of phenyl ring in the dithiocarbamate ligand, and also confirms that the functionalizaton of the N-bound organic moiety in dithiocarbamate ligand influences the properties of the complexes.

Optimized structure

The geometry of complex **11** is fully optimized by the HF/LANL2DZ method using the Gaussian09 software. Some important experimental and theoretical geometric parameters are listed in **Table 4** and are in accordance with the atom numbering scheme given in the ORTEP view of the compound (**Fig**. **6)**. Bond lengths and bond angles obtained from the single crystal X-ray structure determination are compared with their optimized counterparts. It can be seen that the calculated structural parameters for complex in the gas phase are in good agreement with the structure determined by X-ray crystallography in the solid state except Ni-S and Ni-P distances. Comparison of the experimental bond parameters with the calculated values shows that the bond length difference is 0.079 Å and 0.020 Å for C-S and C-N distances and bond angle difference is 3.84° (C12-N2-Ni1). The difference in Ni-S and Ni-P bond distances is 0.222 Å (Ni-S1) and 0.331 (Ni-P1), respectively. This indicates the absence of *trans* influence and back bonding interaction between Ni and P in gaseous state.

HOMO-LUMO

The HOMO–LUMO gap energy is an important parameter which characterizes the electronic structure of molecules and is also used to determine their kinetic stability (reactivity) and electrical conductivity [56]. From the MO’s plot (Fig.7), it can be seen that the HOMO is mainly centered on the **P** atom of the triphenylphosphine and on the metal coordinated sulfur atom (which act as donor atoms) whereas the LUMO is mainly located over the **N** and **S** atoms of the thiocyanate fragment (which function as acceptor atoms).

HOMO energy = -8.1110 eV

LUMO energy = 1.8206 eV

HOMO-LUMO energy gap = -6.2904 eV

The energy gap between the HOMO and LUMO are related to the hardness of a molecule, η, which is defined as: $\eta = (I\text{-}A)/2$. Where I and A are the ionization potential and the electron affinity of the system, respectively. The hardness of complex **11** is then calculated as -3.452 eV.

Molecular Electrostatic Potential (MEP) surface

The MEP surface was obtained at the HF/LANL2DZ optimized geometry to predict reactive sites for electrophilic attack and nucleophilic reaction processes for the complex. Molecular electrostatic potential surface map of complex **11** is given in **Fig. 8**. The negative and positive regions of the MEP are related to electrophilic and nucleophilic regions of the compound, respectively. The negative regions are indicated by red and yellow and positive regions are represented in blue colour

(**Fig. 8**). From the figures, it can be concluded that this molecule has several possible sites for electrophilic attack. The negative regions are mainly over the thiocyanate sulfur (-6.669). Thus, it is predicted that an electrophile would preferentially attack the thiocyanate sulfur atom [57, 58]. The positive charge (dark blue) on the nitrogen atom **N1,** and the negative charge (light yellow) on the **C1**, **S1** and **S2** atoms of dithiocarbamate group, indicate a partial the double bond character of the formally single N-C bond (Fig. **9**) in the dithiocarbmate moiety.

Conclusion

Complexes **1-12** were prepared and characterized by IR, UV-Vis, and NMR spectroscopy. IR and ^{13}C NMR spectral studies showed the increase in the double bond character of the thioureide C-N bond in heteroleptic complexes, due to the presence of the triphenylphosphine group. Anagostic and C-H···F (polymeric structure) interactions are observed in complex **11**. These interactions are totally absent in (N-cyclopropyl-N-benzyldithiocarbamato-S,S′)(thiocyanato-N)(triphenylphosphine)nickel(II). This confirms that functionalization of the dithiocarbamate ligand might increases the inter- and intramolecular interactions. The molecular geometry, HOMO-LUMO and MEP have been calculated, the latter also supporting the partial double bond character of the C-N thioureide bond in the dithiocarbamate fragment.

Supplementary data

Crystallographic data for the structure reported in this paper have been deposited in the Cambridge Crystallographic Data Centre, as supplementary publication CCDC No.-1057195 (complex **11)**. Copies of the data can be obtained free of charge from the CCDC, 12 Union Road, Cambridge CB1 1EZ, UK (Tel: (+44) 1223-336-408; Fax: (+44) 1223-336-003; E-mail: deposit@ccdc.cam.ac.uk).

References

[1]. D. Bouvet, A. Michalowicz, S. Crauste-Manciet, D. Brossard, K. Provost, Inorg. Chem., 45 (2006) 3393.

[2]. L. Ronconi, L. Giovagnini, C. Marzano, F. Bettı`o, R. Graziani, G. Pilloni, D. Fregona, Inorg. Chem., 44 (2005) 1867.

[3]. Md. K. Nazeeruddina, S.M. Zakeeruddin, J.-J. Lagref, P. Liska, P. Comte, C. Barolo, G. Viscardi, K. Schenk, M. Graetzel, Coord. Chem. Rev., 248 (2004) 1317.

[4]. D. Chatterjee, S.K. Moulik, L. Giribabu, R. Kanaparthi, Transition Met Chem., (2014), 39, 641.

[5]. P.J. Heard. Prog. Inorg. Chem., 53 (2005) 71.

[6]. S. Fujii, T. Yoshimura, Coord. Chem. Rev. 198 (2000) 89.

[7]. M.J. Cox, E.R.T. Tiekink, Rev. Inorg. Chem. 17 (1997) 1.

[8]. R.S Graniger, P. Innocenti, Heteroat.Chem, 18 (2007) 568.

[9]. E. Sathiyaraj, S. Thirumaran, Spectrochim. Acta A, 97 (2012) 575.

[10]. M.D. Regulacio, N. Tomson, S.L. Stoll, Chem. Mater., 17 (2005) 3114.

[11]. N. Srinivasan, S. Thirumaran, Superlattices and Microstructures, 51 (2012) 912.

[12]. K. Ramasamy, M.A. Malik, P. O'Brien, J. Raftery, Dalton Trans., 39 (2010) 1460.

[13]. B. Arul Prakasam, M. Lahtinen, A. Peuronen, M. Muruganandham, E. Kolehmainen, E. Haapaniemi, M. Sillanpaa, Polyhedron, 81 (2014) 588.

[14]. R. Chauhan, M. Trivedi, J. Singh, K.C. Molloy, G. Kociok-Kohn, U.P. Mulik, D.P. Amalnerkar and A. Kumar, Inorg. Chim. Acta., 415 **(**2014) 69.

[15]. P. O'Brien and J. Waters, Chem. Vap. Deposition, **12** (2006) 620.

[16]. N. Srinivasan, P. Valarmathi, S. Thirumaran, S. Ciattini, Trans. Metal Chem., 35 (2010) 815.

[17]. C. Anastasiadis, G. Hogarth, J.D.E.T. Wilton-Ely, Inorg. Chim. Acta, 363 (2010) 3222.

[18]. S. Srinivasan, K. Ramalingam, C. Rizzoli, Z. Anorgallg. Chem, 638 (2012) 1356.

[19]. K. Oliver, A.J.P. White, G. Hogarth and J.D.E.T. Wilton-Ely, Dalton Trans., 2011, *40*, 5852.

[20]. E.R.T. Tiekink and J.-Z. Schpector, Chem. Commun., **2011**, *47*, 6623.

[21]. J.D.E.T. Wilton-Ely, D. Solanki, E.R. Knight, K.B. Holt, A.L. Thompson and G. Hogarth, Inorg. Chem., **2008**, *47*, 9642.

[22]. B.G. Sejekan, G. Aravamudan, Monat. Chemie 109 (1978) 165.

[23]. S. Thirumaran, V. Venkatachalam, A. Manohar, K. Ramalingam, G. Bocelli, A. Cantoni, J. Coord. Chem., 44 (1998) 281.

[24]. Y. Han, H.V. Huynh, L.L.J. Koh, Organomet. Chem. 692 (2007) 3606.

[25]. Y. Han, H.V. Huynh, G.K. Tan, Organometallics, 26 (2007) 4612.

[26]. N. Singh, B. Singh, S.K. Singh, M.G.B. Drew, Inorg. Chem. Commun., 13 (2010) 1451.

[27]. B. Singh, M.G.B. Drew, G.K. Kohn, K.C. Molloy, N. Singh, Dalton Trans., 40 (2011) 623.

[28]. S.K. Singh, K. Diwan, M.G.B. Drew and N. Singh, Inorg. Chim. Acta, 384 (2012) 176.

[29]. R. Angamuthu, L.L. Gelauff, M.A. Siegler, A.L. Spek, E. Bouwman, Chem. Commun., (2009) 2700.

[30]. M. Brookhart, M.L.H Green, G. Parkin, Proc. Natl. Acad. Sci.U.S.A, 104 (2007) 6909.

[31]. S.K. Singh, M.G.B. Drew, N. Singh, Cryst Eng Comm, 15 (2013) 10255.

[32]. H.V. Huynh, L.R. Wong, P. Shuyi Ng, Organometallics, 27 (2008) 2231.

[33]. C. Ravikumar, I.H. Joe, V.S. Jayakumar, Chem. Phys. Lett. 460 (2008) 552.

[34]. Y.X. Sun, Q.L. Hao, L.D. Lu, X. Wang, X.J. Yang, Spectrochim. Acta Part A., 75 (2010) 203.

[35]. S. Çetin, G. Yildirim, C. Parlak, M. Akdogan, C. Terzioglu, Spectrochim. Acta Part A., 79 (2011) 1024.

[36]. G. M. Sheldrick, Acta Crystallogr., Sect. A: Found. Crystallogr., 46 (1990) 467.

[37]. G. M. Sheldrick, SHELXL-97, University of Gottingen, (1997), Gottingen, Germany.

[38]. M.J. Frisch, G.W. Trucks, H.B. Schlegel, G.E. Scuseria, M.A. Robb, J.R. Cheeseman, G. Scalmani, V. Barone, B. Mennucci, G.A. Petersson, H. Nakatsuji, M. Caricato, X. Li, H.P. Hratchian, A.F. Izmaylov, J. Bloino, G. Zheng, J.L. Sonnenberg, M. Hada, M. Ehara, K. Toyota, R. Fukuda, J. Hasegawa, M. Ishida, T. Nakajima, Y. Honda, O. Kitao, H. Nakai, T. Vreven, J.A. Montgomery Jr., J.E. Peralta, F. Ogliaro, M. Bearpark, J.J. Heyd, E. Brothers, K.N. Kudin, V.N. Staroverov, R. Kobayashi, J. Normand, K. Raghavachari, A. Rendell, J.C. Burant, S.S. Iyengar, J. Tomasi, M. Cossi, N. Rega, J.M. Millam, M. Klene, J.E. Knox, J.B. Cross, V. Bakken, C. Adamo, J. Jaramillo, R. Gomperts, R.E. Stratmann, O. Yazyev, A.J. Austin, R. Cammi, C. Pomelli, J.W. Ochterski, R.L. Martin, K. Morokuma, V.G. Zakrzewski, G.A. Voth, P. Salvador, J.J. Dannenberg, S. Dapprich, A.D. Daniels, Ö. Farkas, J.B. Foresman, J.V. Ortiz, J. Cioslowski, D.J. Fox, Gaussian Inc., Wallingford CT, Gaussian 09, Revision D.01, 2009.

[39]. G. Hogarth, Transition Metal Dithiocarbamates: 1978–2003, in Progress in Inorganic Chemistry, Volume 53 (Ed. K. D. Karlin), 2005, John Wiley & Sons Inc, Hoboken, NJ, USA and references cited therein

[40]. Z. Travnicek, R. Pastorek, V. Slovak, Polyhedron, 27 (2008) 411.

[41]. M. Altaf, M. Monim-ul-Mehboob, Adam A.A. Seliman, M. Sohail, Mohammed I.M. Wazeer, Anvarhusein A. Isab, L. Li, V. Dhuna, G. Bhatia, K. Dhuna., Eur. J. Med. Chem., DOI: 10.1016/j.ejmech.2015.03.019

[42]. I. Ozturk, C.N. Banti, N. Kourkoumelis, M.J. Manos, A.J. Tasiopoulos, A.M. Owczarzak, M. Kubickie , S.K. Hadjikakou, Polyhedron., 67 (2014) 89.

[43]. P. Valarmathi, N. Srinivasan and S. Thirumaran., J. Sulfur Chem., 32 (2011), 583.

[44]. F. Bonati, R. Ugo, J. Organomet. Chem. 10 (1967) 257.

[45]. C.K. Jorgensen, J. Inorg. Nucl. Chem. 24 (1962) 1571.

[46]. R. Pastorek, J. Kmenick, Z. Trawnick, J. Husaret, N. Dutty, Polyhedron., 18 (1999) 2879.

[47]. P. Valarmathi, S. Thirumaran, L. Sarmal, Rajni Kant., Spectrochimica Acta Part A: 129 (2014) 285.

[48]. H.C.M. Van Gael, J.W. Diesveld, F.W. Pijpans, J.G.M. Van der Lin don, Inorg. Chem., **18** (1979), 3251.

[49]. R.M. Silver stein, F.X. Webster, Spectrometric identification of organic compounds, sixth edition, 2006.

[50]. L.Yang, D.R. Powell, R.P. Houser, Dalton Trans. 2007, 955.

[51]. P. Jamuna Rani, S Thirumaran, S. Ciattini, Phosphorus, Sulfur Silicon Relat. Elem., 188 (2013) 778.

[52]. L. Brammer, Dalton Trans. (2003) 3145.

[53]. J. C. Lewis, J. Wu, R. G. Bergman and J. A. Ellman, Organometallics., 24 (2005) 5737.

[54]. S. K. Singh, M. G. B. Drewb, N Singh, Cryst.Eng.Comm, 15 (2013) 10255.

[55]. E. Sathiyaraj, P Valarmathi, S. Thirumaran, S. Ciattini, V.K. Gupta and Rajni Kant, Phosphorus Sulfur Silicon Relat. Elem., 190, (2015), 1127.

[56]. I. Fleming, Frontier Orbitals and Organic Chemical Reactions, Wiley, London, 1976.

[57]. V. Balachandran, G. Santhi, V. Karpagam, A. Lakshmi, J. Mol. Struct.,1047 (2013) 249.

[58]. V.P. Gupta, A. Sharma, V. Virdi, V.J. Ram, Spectrochim. Acta A 64 (2006) 57.

Figure captions

Fig. 1. Structure of complexes

Fig. 2. ORTEP of complex **11**

Fig. 3. Intramolecular S···H–C interaction in complex **11**

Fig. 4 Polymeric chain through intermolecular C-H···F interactions

Fig. 5. Intramolecular Ni···H-C anagostic interaction in complex **11**

Fig. 6. Optimized structure of complex **11**

Fig. 7. The frontier molecular orbital (HOMO-LUMO) pictures of the optimized complex **11**

Fig. 8. Molecular electrostatic potential surface map of complex **11**

Fig. 9. Resonance forms of dithiocarbamate

Table 1. Data Refinement Parameters for complex

Empirical formula	$C_{30} H_{26} F N_2 Ni P S_3$
FW	619.39
Crystal dimensions (mm)	$0.30 \times 0.25 \times 0.20$
Crystal system	Monoclinic
Space group	P 21/n
a/Å	14.227(5)
b/Å	9.947(5)
c/Å	21.271(5)
α/°	90.000
β/°	102.721(5)
γ/°	90.000
V/Å^3	2936.3(19)
Z	4
Dc/g cm^{-3}	1.388
μ/cm^{-1}	0.957
F(000)	1280
λ/Å	MoK$_\alpha$ (0.71073)
θ Range/°	1.58-28.37
Index ranges	$-19 \leq h \leq 18$, $-13 \leq k \leq 13$, $-26 \leq l \leq 28$
Reflections collected	28037
Observed reflections I > 2σ(I)	4839
Weighting scheme	Calc. $W = 1/(\sigma^2(F_o^2) + (0.0791p)^2 + 2.4944p)$ where $p = (F_o^2 + 2F_c^2)/3$
Number of parameters refined	343
$R[F^2 > 2\sigma(F^2)]$, $wR(F^2)$	0.0527, 0.1380
GOOF	1.061

Table 2. Selected bond distances (Å) and angles (°) for complex **11**

Bond distances (Å)	XRD	Bond angles (°)	XRD
C1-N1	1.314(4)	N1-C1-S1	126.8(3)
C1-S1	1.709(3)	N1-C1-S2	124.5(3)
C1-S2	1.725(3)	S1-C1-S2	108.63(19)
C12-N2	1.147(5)	N2-C12-S3	178.6(4)
C12-S3	1.609(4)	C12-N2-Ni1	170.3(4)
N2-Ni1	1.859(3)	N2-Ni1-P1	95.13(10)
P1-Ni1	2.1991(12)	N2-Ni1-S1	93.45(10)
S1-Ni1	2.2234(12)	S2-Ni1-S1	78.55(4)
S2-Ni1	2.1819(11)	S1-Ni1-P1	92.73(4)

Table 3. Distances (Å) and angles (°) of the hydrogen bond interactions in complex **11**

Interactions	D-H	H···A	D···A	D-H···A
C4-H4B···S1[a]	0.970	2.619	3.078	109.23
C3-H3B···F1[b]	0.970	2.441	3.345	154.81
C1-H1···F1[b]	0.986	2.352	3.311	165.85
C24-H24···Ni[a]	0.931	2.929	3.455	117.13

[a] Intramolecular contacts.

[b] Intermolecular contacts.

Table 4. Selected bond distances (Å) and angles (°) for complex **11**

Bond distances (Å)	XRD	HF/LAN2DZ	Bond angles (°)	XRD	HF/LAN2DZ
C1-N1	1.314(4)	1.320	N1-C1-S1	126.8(3)	123.12
C1-S1	1.709(3)	1.788	N1-C1-S2	124.5(3)	124.40
C1-S2	1.725(3)	1.782	S1-C1-S2	108.63(19)	112.46
C12-N2	1.147(5)	1.167	N2-C12-S3	178.6(4)	178.20
C12-S3	1.609(4)	1.676	C12-N2-Ni1	170.3(4)	174.14
N2-Ni1	1.859(3)	1.893	N2-Ni1-P1	95.13(10)	92.57
P1-Ni1	2.1991(12)	2.531	N2-Ni1-S1	93.45(10)	95.50
S1-Ni1	2.2234(12)	2.379	S2-Ni1-S1	78.55(4)	76.68
S2-Ni1	2.1819(11)	2.404	S1-Ni1-P1	92.73(4)	95.15

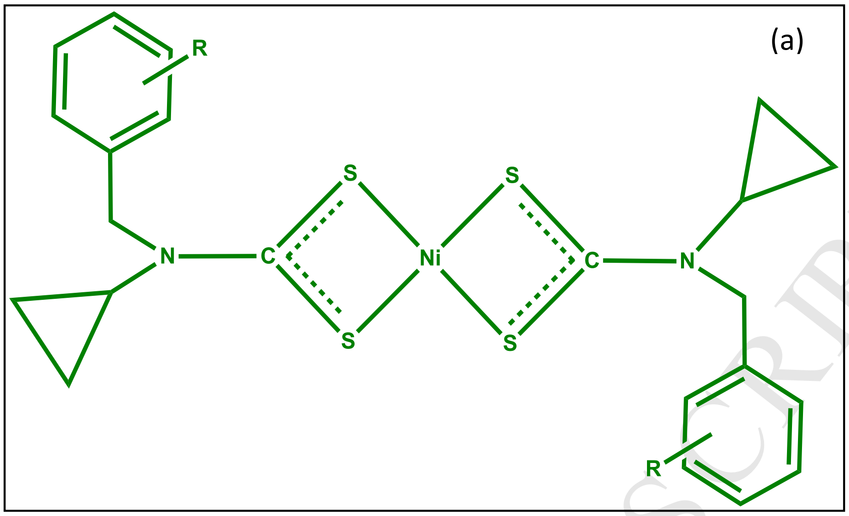

1-6

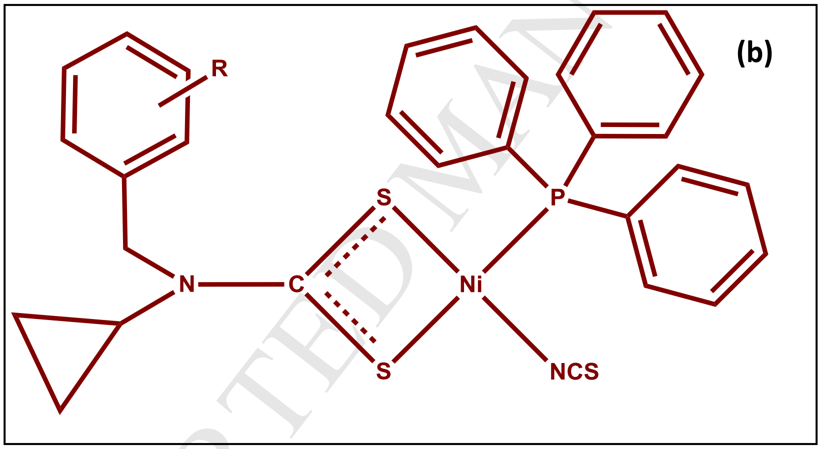

7-12

Fig. 1.

Complex	Substituent (R)
1, 7	2-OH
2, 8	3-OH
3, 9	4-OH
4, 10	4-OCH_3
5, 11	4-F
6, 12	4-Cl

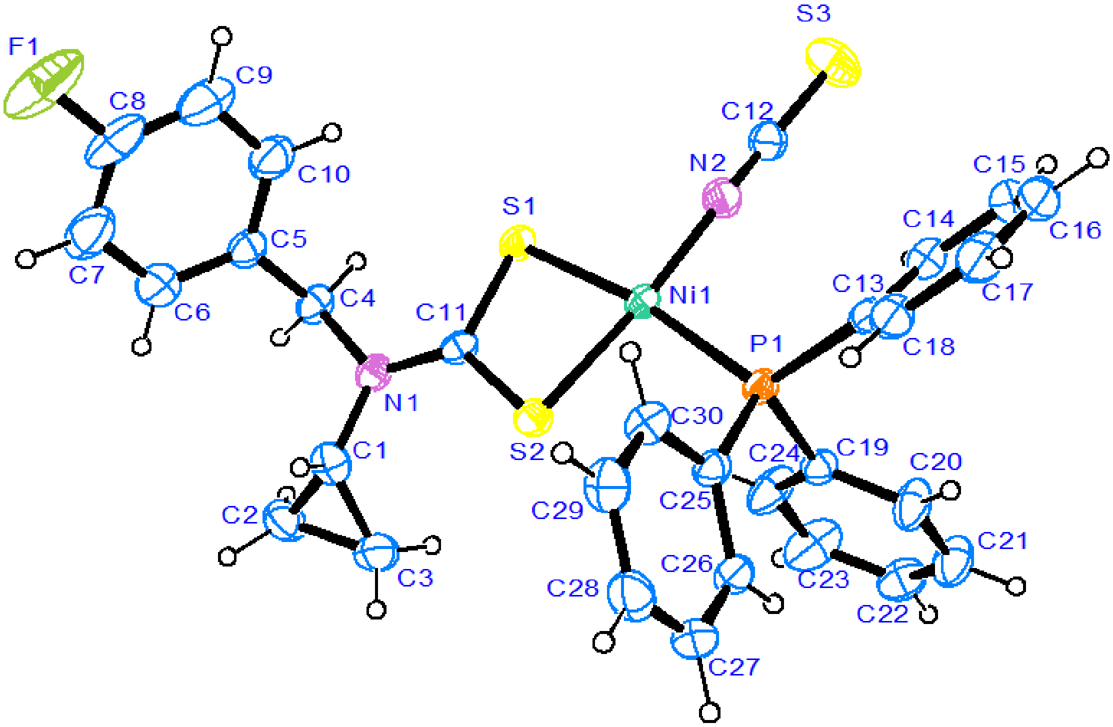
F1
C9
C8
C10
C7
C6
C5
C4
C11
S1
S3
C12
N2
Ni1
C15
C16
C14
C17
C13
C18
P1
N1
S2
C30
C1
C2
C3
C29
C25
C24
C19
C20
C21
C26
C23
C28
C22
C27

Fig. 2.

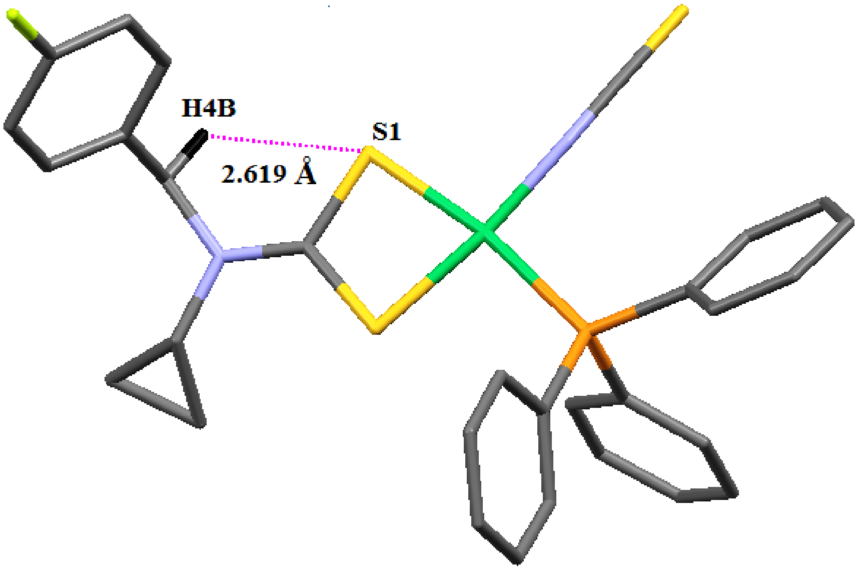

Fig. 3.

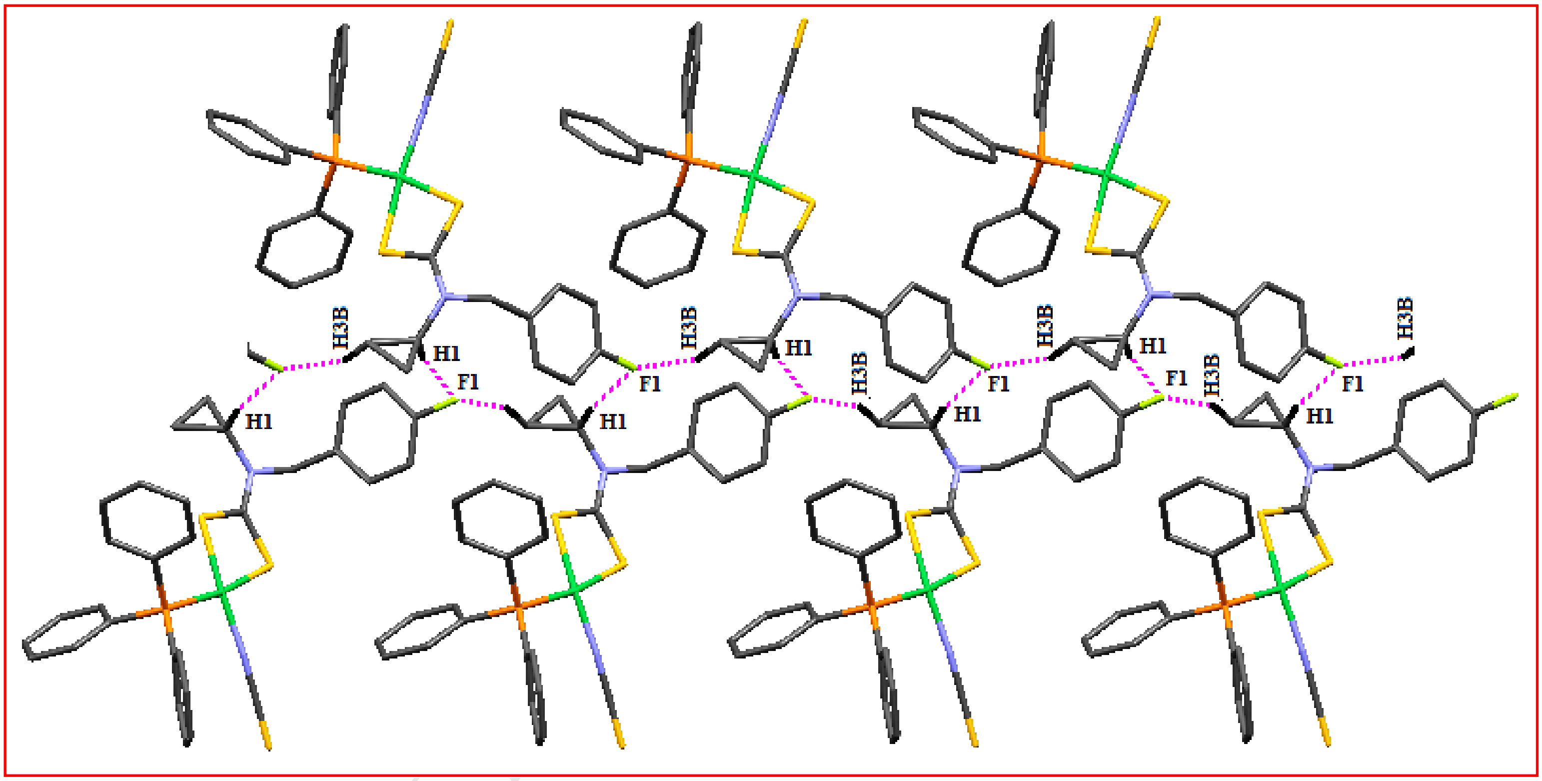

Fig. 4.

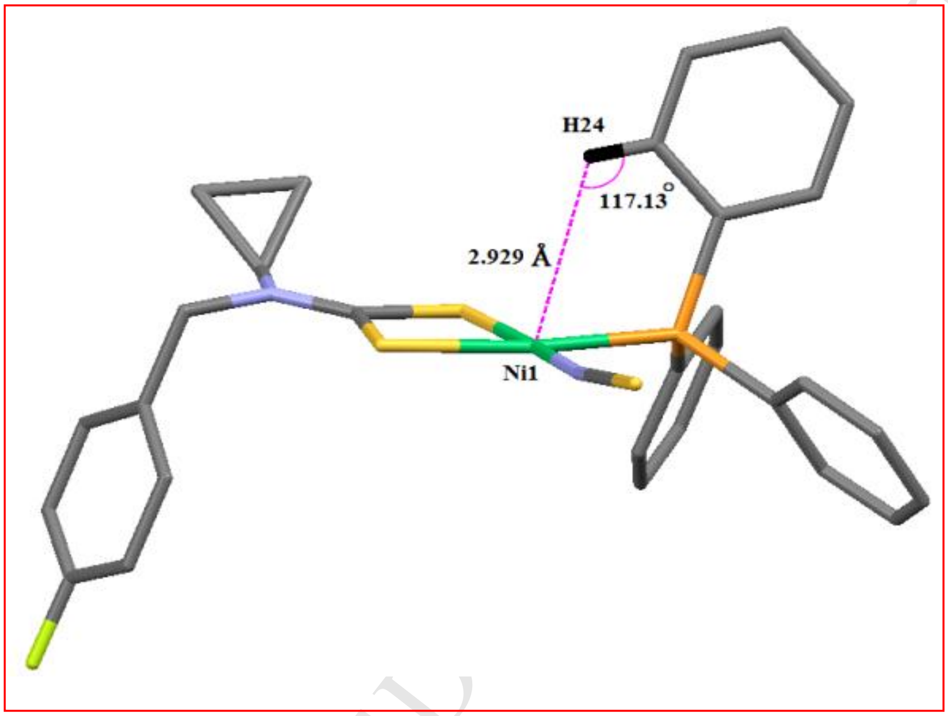

Fig. 5.

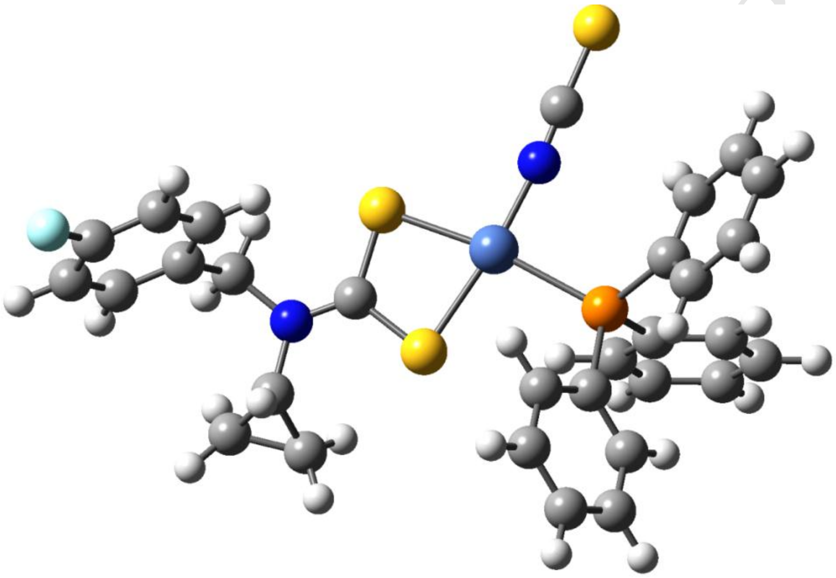

Fig. 6.

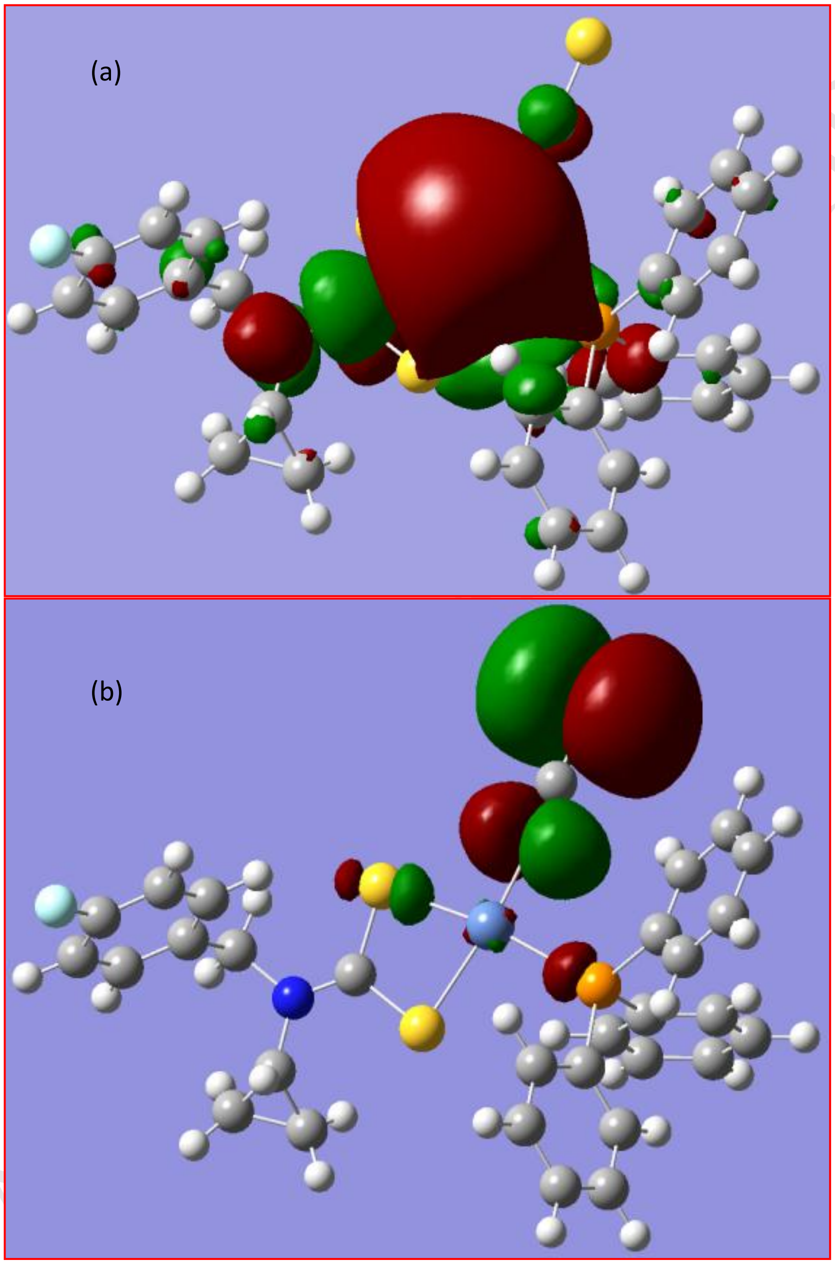

Fig. 7.

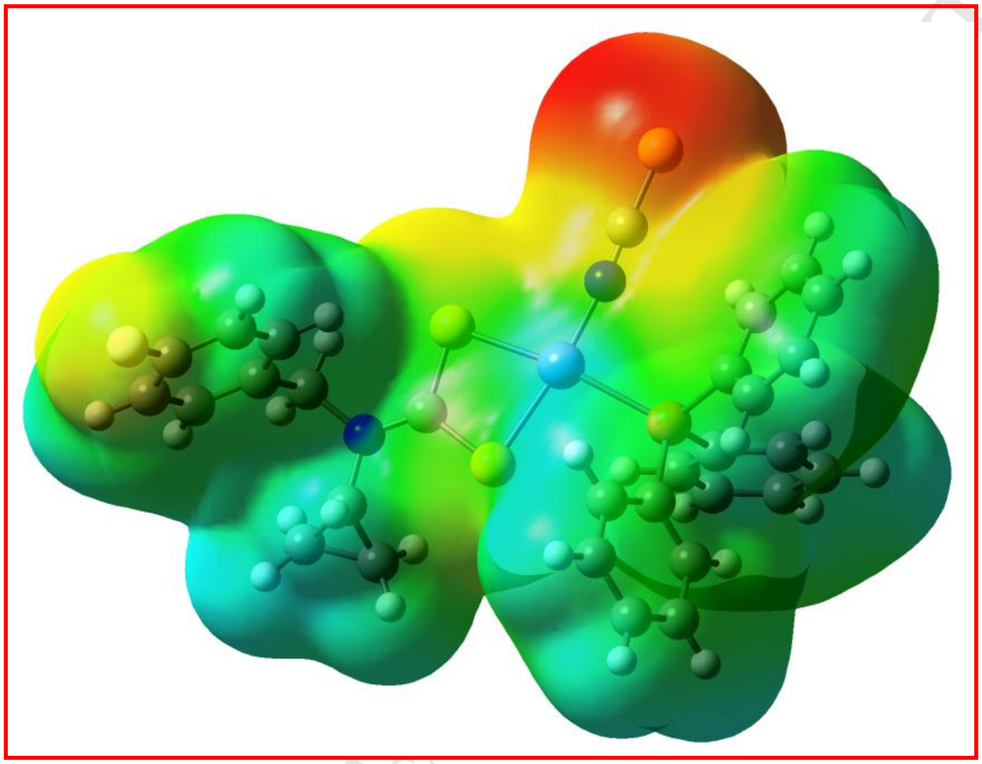

Fig. 8.

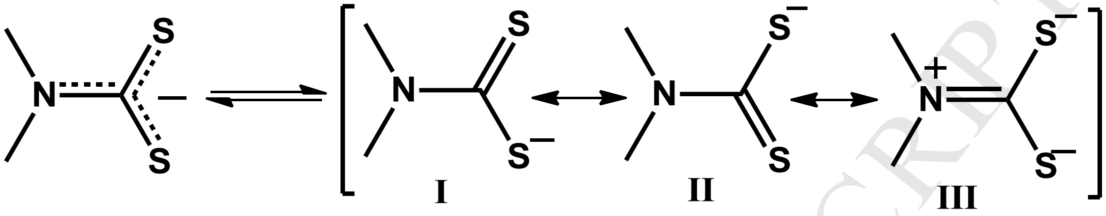

Fig. 9.

Highlights

Twelve new nickel(II) complexes involving S and P donor ligands were synthesized.

Rare intramolecular anagostic interaction (Ni···H=2.929Å) was observed.

C-H···F interactios result in the polymeric chain structure.

The optimized bond parameters agree well with the experimental results.

Synthesis and spectroscopic characterization of Ni(II) complexes involving functionalised dithiocarbamates and triphenylphosphine: anagostic interaction in (N-cyclopropyl-N-(4-fluorobenzyl)dithiocarbamato-S,S′)-(thiocyanato-N)(triphenylphosphine)nickel(II)

E. Sathiyaraj[a], T. Srinivasan[b], S. Thirumaran[a]* and D. Velmurugan[b]

Journal of molecular structure

Complex **1**

Yield 71%, mp 208-212°C, IR (KBr, cm^{-1}): ν = 3298 (ν_{OH}); 1474 ($\nu_{C–N}$); 1030 ($\nu_{C–S}$). UV-Vis (CH_3CN, nm): λ = 601, 444, 400, 333, 252. ^{1}H NMR (400 MHz, DMSO, ppm): δ = 4.68 (s, 2HO–C_6H_4–C$\boldsymbol{H_2}$–N); 2.79 (s, N–C$\boldsymbol{H}$ (^{c}Pr)); 0.77-0.86 (m, C$\boldsymbol{H}_2$ (^{c}Pr)); 9.84 (s, 2$\boldsymbol{H}$O–C_6H_4–CH_2–N); 6.83-7.15 (aromatic protons).^{13}C NMR (100 MHz, $CDCl_3$, ppm): δ = 7.8 ($\boldsymbol{C}H_2$ (^{c}Pr)); 31.8($\boldsymbol{C}$H (^{c}Pr)); 53.1 (C_6H_5–$\boldsymbol{C}H_2$–N); 127.9-134.9 (aromatic carbons); 212.8 (N$\boldsymbol{C}S_2$); Anal. Calcd. for Chemical Formula: $C_{22}H_{24}N_2NiO_2S_4$ (%): Elemental Analysis: C, 49.35; H, 4.52; N, 5.23; Found: C, 49.10; H, 4.48; N, 5.14.

Complex **2**

Yield 69%, mp 181-183°C. IR (KBr, cm^{-1}): ν =3387 (ν_{OH}); 1472 ($\nu_{C–N}$); 1030 ($\nu_{C–S}$). UV-Vis (CH_3CN, nm): λ = 622, 443, 400, 326, 276, 249. ^{1}H NMR (400 MHz, DMSO, ppm): δ = 4.66 (s, 3HO–C_6H_4–C$\boldsymbol{H_2}$–N); 2.71 (s, N–C$\boldsymbol{H}$ (^{c}Pr)); 0.84 (b, C$\boldsymbol{H}_2$ (^{c}Pr)); 9.77 (s, 3$\boldsymbol{H}$O–C_6H_4–CH_2–N); 6.64-7.20 (aromatic protons);^{13}C NMR (100 MHz, $CDCl_3$, ppm): δ =7.0 ($\boldsymbol{C}H_2$ -^{c}Pr); 32.1($\boldsymbol{C}$H -^{c}Pr); 47.9 (2HO–C_6H_4–$\boldsymbol{C}H_2$–N); *ipso carbon*; 154.8 (Ar-2OH); 115.1-128.7 (other aromatic carbons); 209.7 (N$\boldsymbol{C}S_2$).; Anal. Calcd. for Chemical Formula: $C_{22}H_{24}N_2NiO_2S_4$ (%): Elemental Analysis: C, 49.35; H, 4.52; N, 5.23; Found: C, 49.16; H, 4.52; N, 5.10

Complex **3**

Yield 67%, mp 172-178°C. IR (KBr, cm^{-1}): ν =3391 (ν_{OH}); 1474 ($\nu_{C–N}$); 1026 ($\nu_{C–S}$). UV-Vis (CH_3CN, nm): λ = 621, 478, 394, 326, 275, 266, 240.^{1}H NMR (400 MHz, DMSO, ppm): δ = 4.65 (s, 4HO–C_6H_4–C$\boldsymbol{H_2}$–N); 2.61 (s, N–C$\boldsymbol{H}$(^{c}Pr)); 0.81-0.89 (m, C$\boldsymbol{H}_2$ (^{c}Pr)); 9.58 (s, 4$\boldsymbol{H}$O–C_6H_4–CH_2–N); 6.77-7.14 (aromatic protons);^{13}C NMR (100 MHz, $CDCl_3$, ppm): δ =7.2 ($\boldsymbol{C}H_2$-^{c}Pr); 31.5($\boldsymbol{C}$H-^{c}Pr); 51.8 (4HO–C_6H_4–$\boldsymbol{C}H_2$–N); *ipso carbon*; 157.1 (Ar-4OH);

115.4-129.1 (other aromatic carbons); 209.1 ($N\boldsymbol{C}S_2$). Anal. Calcd. for Chemical Formula $C_{22}H_{24}N_2NiO_2S_4$ (%): Elemental Analysis: C, 49.35; H, 4.52; N, 5.23; Found: C, 49.02; H, 4.43; N, 5.21.

Complex **4**

Yield 75%, mp 200-202°C. IR (KBr, cm^{-1}): ν = 1470 ($\nu_{C–N}$); 1028 ($\nu_{C–S}$). UV-Vis ($CHCl_3$, nm): λ = 628, 454, 403, 347, 339, 261. ^1H NMR (400 MHz, $CDCl_3$, ppm): δ = 4.72 (s, $4CH_3O–C_6H_4–C\boldsymbol{H_2}–N$); 3.82 (s, $4C\boldsymbol{H}_3O–C_6H_4–CH_2–N$); 2.62 (s, $N–C\boldsymbol{H}$ (^{c}Pr)); 0.88-0.89 (m, $C\boldsymbol{H}_2$ (^{c}Pr)); 6.88-7.26 (aromatic protons); ^{13}C NMR (100 MHz, $CDCl_3$, ppm): δ =7.8 ($\boldsymbol{C}H_2$ -^{c}Pr); 31.5 ($\boldsymbol{C}H$ -^{c}Pr); 52.5 ($4CH_3O–C_6H_4–\boldsymbol{C}H_2–N$); 55.4 ($4\boldsymbol{C}H_3O–C_6H_4–\boldsymbol{C}H_2–N$); *ipso carbon*; 159.4 (Ar-$4O\boldsymbol{C}H_3$); 114.2-129.4 (other aromatic carbons); 212.3 ($N\boldsymbol{C}S_2$). Anal. Calcd. for Chemical Formula: $C_{24}H_{28}N_2NiO_2S_4$ (%): Elemental Analysis: C, 51.16; H, 5.01; N, 4.97; Found: C,51.20; H,4.89; N, 4.90.

Complex **5**

Yield 76%, mp 146-149°C. IR (KBr, cm^{-1}): ν = 1472 ($\nu_{C–N}$); 1022 ($\nu_{C–S}$). UV-Vis ($CHCl_3$, nm): λ = 622, 403, 353, 323, 305, 264. ^1H NMR (400 MHz, $CDCl_3$, ppm): δ =4.76 (s, $4F–C_6H_4–C\boldsymbol{H_2}–N$); 2.64 (s, $N–C\boldsymbol{H}$ (^{c}Pr)); 0.89 (s, $C\boldsymbol{H}_2$ (^{c}Pr)); 7.06-7.32 (aromatic protons); ^{13}C NMR (100 MHz, $CDCl_3$, ppm): δ =7.8 ($\boldsymbol{C}H_2$-^{c}Pr); 31.6($\boldsymbol{C}H$-^{c}Pr); 52.3 ($4F–C_6H_4–\boldsymbol{C}H_2–N$); *ipso carbon*; 161.3, 163.7 (Ar-4F); 114.6-130.7 (other aromatic carbons); 212.9 ($N\boldsymbol{C}S_2$). Anal. Calcd. for Chemical Formula: $C_{22}H_{22}F_2N_2NiS_4$ (%): Elemental Analysis: C, 48.99; H, 4.11; N, 5.19; Found: C, 48.68; H, 4.02; N, 5.21.

Complex **6**

Yield 71%, mp 204-206°C. IR (KBr, cm^{-1}): ν = 1472 ($\nu_{C–N}$); 1005 ($\nu_{C–S}$). UV-Vis ($CHCl_3$, nm): λ = 631, 449, 402, 337, 291, 258. ^1H NMR (400 MHz, $CDCl_3$, ppm): δ =4.75 (s, $4Cl–C_6H_4–$

C***H₂***–N); 2.66 (s, N–C***H*** (^{c}Pr)); 0.89 (s, C***H***$_2$ (^{c}Pr)); 7.27-7.35 (aromatic protons); ^{13}C NMR (100 MHz, CDCl$_3$, ppm): δ =7.8 (***C***H$_2$ -^{c}Pr); 31.7 (***C***H -^{c}Pr); 52.4 (4Cl–C$_6$H$_4$–***C***H₂–N); 129.1-134.0 (aromatic carbons); 213.1 (N***C***S$_2$). Anal. Calcd. for Chemical Formula: $C_{22}H_{22}Cl_2N_2NiS_4$ (%): Elemental Analysis: C, 46.17; H, 3.87; N, 4.90; Found: C, 46.00; H, 3.81; N, 4.81.

Complex **7**

Yield 68%, mp 104-106°C. IR (KBr, cm^{-1}): ν = 3289 (ν_{OH}); 2093 ($\nu_{(NCS)}$); 1487 ($\nu_{C–N}$); 1028 ($\nu_{C–S}$). UV-Vis (CH$_3$CN, nm): λ =484, 333, 249. ^{1}H NMR (400 MHz, CDCl$_3$, ppm): δ =4.56-4.79 (bd, 2HO–C$_6$H$_4$–C***H₂***–N); 2.53, 2.66 (bd, N–C***H*** (^{c}Pr)); 0.66-0.82 (m, C***H₂*** (^{c}Pr)); 6.87-7.69 (aromatic protons); ^{13}C NMR (100 MHz, CDCl$_3$, ppm): δ = 5.4, 5.8 (***C***H$_2$-^{c}Pr); 29.8, 29.9 (***C***H-^{c}Pr); 46.2 (2OH−C$_6$H$_4$–***C***H₂–N); *ipso carbon*; 152.4, 152.5 (Ar-2OH); 114.2-132.2 (other aromatic carbons); 141.2(N***C***S); 206.1 (N***C***S$_2$). Anal. Calcd. for Chemical Formula: $C_{30}H_{27}N_2NiOPS_3$ (%): Elemental Analysis: C, 58.36; H, 4.41; N, 4.54; Found: C, 58.03; H, 4.42; N, 4.49.

Complex **8**

Yield 65 %, mp 163-165°C. IR (KBr, cm^{-1}): ν = 3408 (ν_{OH}); 2089 ($\nu_{(NCS)}$); 1483 ($\nu_{C–N}$); 1028 ($\nu_{C–S}$). UV-Vis (CH$_3$CN, nm): λ =480, 333, 251. ^{1}H NMR (400 MHz, CDCl$_3$, ppm): δ = 4.52 (b, 3HO–C$_6$H$_4$–C***H₂***–N); 2.54 (b, N–C***H*** (^{c}Pr)); 0.76 (b, C***H***$_2$ (^{c}Pr)); 6.64-7.67 (aromatic protons); ^{13}C NMR (100 MHz, CDCl$_3$, ppm): δ = 7.4, 7.6 (***C***H$_2$-^{c}Pr); 31.8(***C***H -^{c}Pr); 53.2 (3HO–C$_6$H$_4$–***C***H₂–N); *ipso carbon*; 157.5 (Ar-3OH); 115.2-135.3 (other aromatic carbons); 208.7 (N***C***S$_2$). Anal. Calcd. for Chemical Formula: $C_{30}H_{27}N_2NiOPS_3$ (%): Elemental Analysis: C, 58.36; H, 4.41; N, 4.54; Found: C, 58.06; H, 4.40; N, 4.54.

Complex **9**

Yield 60%, mp 154-157°C. IR (KBr, cm^{-1}): ν = 3302 (ν_{OH}); 2093 (ν_{NCS}); 1487 ($\nu_{C–N}$); 1026 ($\nu_{C–S}$). UV-Vis (CH_3CN, nm): λ =484, 452, 329, 250, 243. ^{1}H NMR (400 MHz, $CDCl_3$, ppm): δ =4.58 (b, $4HO–C_6H_4–C\boldsymbol{H_2}–N$); 2.49, 2.48 (b, $N–C\boldsymbol{H}(^{c}Pr)$); 0.81 (s, $C\boldsymbol{H}_2(^{c}Pr)$); 6.84-7.65 (aromatic protons). ^{13}C NMR (100 MHz, $CDCl_3$, ppm): δ= 7.5 ($\boldsymbol{C}H_2\text{-}^{c}Pr$); 31.5 ($\boldsymbol{C}H\text{-}^{c}Pr$); 52.9 ($4HO–C_6H_4–\boldsymbol{C}H_2–N$); *ipso carbon*; 156.6 (Ar-4OH); 115.9-134.2 (other aromatic carbons); 208.2 ($N\boldsymbol{C}S_2$). Anal. Calcd. for Chemical Formula: $C_{30}H_{27}N_2NiOPS_3$ (%): Elemental Analysis: C, 58.36; H, 4.41; N, 4.54; Found: C, 58.11; H, 4.33; N, 4.41.

Complex **10**

Yield 78%, mp 162-164 °C. IR (KBr, cm^{-1}): ν = 2089 (ν_{NCS}); 1474 ($\nu_{C–N}$); 1028 ($\nu_{C–S}$). UV-Vis ($CHCl_3$, nm): λ =485, 334, 258, 232. ^{1}H NMR (400 MHz, $CDCl_3$, ppm): δ =4.69, 4.49 (bd, $4CH_3O–C_6H_4–C\boldsymbol{H_2}–N$); 3.81 (s, $4C\boldsymbol{H}_3O–C_6H_4–CH_2–N$); 2.59, 2.47 (bd, $N–C\boldsymbol{H}\ (^{c}Pr)$); 0.78, 0.88 (bd, $C\boldsymbol{H}_2\ (^{c}Pr)$); 6.88-7.12 (aromatic protons); ^{13}C NMR (100 MHz, $CDCl_3$, ppm): δ =7.5 ($\boldsymbol{C}H_2\text{-}^{c}Pr$); 31.4 ($\boldsymbol{C}H\text{-}^{c}Pr$); 52.7 ($4CH_3O–C_6H_4–\boldsymbol{C}H_2–N$); 55.4 ($4\boldsymbol{C}H_3O–C_6H_4–\boldsymbol{C}H_2–N$); *ipso carbon;*159.6 ($Ar\text{-}4OCH_3$); 114.3-134.2 (other aromatic carbons); 143.4 ($N\boldsymbol{C}S$); 208.7 ($N\boldsymbol{C}S_2$). Anal. Calcd. for Chemical Formula: $C_{31}H_{29}N_2NiOPS_3$ (%): Elemental Analysis: C, 58.97; H, 4.63; N, 4.44; Found: C, 58.69; H, 4.56; N, 4.40.

Complex **11**

Yield 84%, mp 152-156°C. IR (KBr, cm^{-1}): ν = 2083 (ν_{NCS}); 1491 ($\nu_{C–N}$); 1022 ($\nu_{C–S}$). UV-Vis ($CHCl_3$, nm): λ =482, 401, 332, 253. ^{1}H NMR (400 MHz, $CDCl_3$, ppm): δ =4.69, 4.56 (bd, $4F–C_6H_4–C\boldsymbol{H_2}–N$); 2.51 (b, $N–C\boldsymbol{H}\ (^{c}Pr)$); 0.83 (b, $C\boldsymbol{H}_2\ (^{c}Pr)$), 7.04-7.69 (aromatic protons); ^{13}C NMR (100 MHz, $CDCl_3$, ppm): δ =7.5 ($\boldsymbol{C}H_2\text{-}^{c}Pr$); 31.5 ($\boldsymbol{C}H\text{-}^{c}Pr$); 52.4

(4F–C_6H_4–***C***H_2–N); *ipso carbon*; 161.4, 163.9 (Ar-4F); 115.8-134.2 (aromatic carbons); 209.5 (N***C***S_2). Anal. Calcd. for Chemical Formula: $C_{30}H_{26}FN_2NiPS_3$ (%): Elemental Analysis: C, 58.17; H, 4.23; N, 4.52; Found: C, 58.22; H, 4.14; N, 4.43.

Complex **12**

Yield 79%, mp 161-163°C. IR (KBr, cm^{-1}): ν = 2087 (ν_{NCS}); 1474 ($\nu_{C–N}$); 1007 ($\nu_{C–S}$). UV-Vis ($CHCl_3$, nm): λ =623, 394, 344, 333, 321, 260. ^{1}H NMR (400 MHz, $CDCl_3$, ppm): δ=4.73, 4.52 (bd, 4Cl–C_6H_4–C$\boldsymbol{H_2}$–N); 2.64, 2.48 (bd, N–C***H*** (^{c}Pr)); 0.76, 0.88 (bd, C$\boldsymbol{H}_2$ (^{c}Pr)); 7.1-7.71 (aromatic protons). ^{13}C NMR (100 MHz, $CDCl_3$, ppm): δ =7.5, 7.8 (***C***H_2-^{c}Pr); 31.8, 31.9 (***C***H-^{c}Pr); 52.4 (4Cl–C_6H_4–***C***H_2–N); 128.5-134.2 (aromatic carbons); 209.9 (N***C***S_2). Anal. Calcd. for Chemical Formula: $C_{30}H_{26}ClN_2NiPS_3$ (%): Elemental Analysis: C, 56.67; H, 4.12; N, 4.41; Found: C, 56.24; H, 4.05 ;N, 4.37.